HYDROLOGICAL PROCESSES
Hydrol. Process. **29**, 4624–4637 (2015)
Published online 6 August 2015 in Wiley Online Library
(wileyonlinelibrary.com) DOI: 10.1002/hyp.10593

Simulating high-resolution soil moisture patterns in the Shale Hills watershed using a land surface hydrologic model

Yuning Shi,[1,5]* Douglas C. Baldwin,[2] Kenneth J. Davis,[1,3] Xuan Yu,[4] Christopher J. Duffy[4] and Henry Lin[5]

[1] *Earth and Environmental Systems Institute, The Pennsylvania State University, University Park, PA, USA*
[2] *Department of Geography, The Pennsylvania State University, University Park, PA, USA*
[3] *Department of Meteorology, The Pennsylvania State University, University Park, PA, USA*
[4] *Department of Civil and Environmental Engineering, The Pennsylvania State University, University Park, PA, USA*
[5] *Department of Ecosystem Science and Management, The Pennsylvania State University, University Park, PA, USA*

Abstract:

Soil moisture is a critical variable in the water and energy cycles. The prediction of soil moisture patterns, especially at high spatial resolution, is challenging. This study tests the ability of a land surface hydrologic model (Flux-PIHM) to simulate high-resolution soil moisture patterns in the Shale Hills watershed (0.08 km^2) in central Pennsylvania. Locally measured variables including a soil map, soil parameters, a tree map, and lidar topographic data, all have been synthesized into Flux-PIHM to provide model inputs. The predicted 10-cm soil moisture patterns for 15 individual days encompassing seven months in 2009 are compared with the observations from 61 soil moisture monitoring sites. Calibrated using only watershed-scale and a few point-based measurements, and driven by spatially uniform meteorological forcing, Flux-PIHM is able to simulate the observed macro spatial pattern of soil moisture at ~10-m resolution (spatial correlation coefficient ~ 0.6) and the day-to-day variation of this soil moisture pattern, although it underestimates the amplitude of the spatial variability and the mean soil moisture. Results show that the spatial distribution of soil hydraulic parameters has the dominant effect on the soil moisture spatial pattern. The surface topography and depth to bedrock also affect the soil moisture patterns in this watershed. Using the National Land Cover Database (NLCD) in place of a local tree survey map makes a negligible difference. Field measured soil type maps and soil type-specific hydraulic parameters significantly improve the predicted soil moisture pattern as compared to the most detailed national soils database (Soil Survey Geographic Database, or SSURGO, 30-m resolution). Copyright © 2015 John Wiley & Sons, Ltd.

KEY WORDS soil moisture pattern; hydrologic model; soil map

Received 8 September 2014; Accepted 21 June 2015

INTRODUCTION

Soil moisture is a critical variable in the water and energy cycles. It determines the partitioning of available energy into sensible, latent, and ground heat fluxes, as well as the partitioning of incoming precipitation into surface runoff and infiltration. Soil moisture is also an important driver of many biogeochemical processes. Capturing the temporal variation and spatial distribution of soil moisture is important for numerical models to accurately simulate land surface, hydrological, and biogeochemical processes.

It is generally held that soil moisture is highly variable in time and space. Many studies have focused on the temporal variation of soil moisture when testing hydrologic models' ability to simulate soil moisture (e.g. Liang *et al.*, 1996; Liang *et al.*, 2003; Livneh *et al.*, 2011; Niu *et al.*, 2011). There are relatively fewer studies examining the spatial patterns of soil moisture predicted by hydrologic models. Western *et al.* (1999) and Western and Grayson (2000) compared the predicted top 30-cm soil moisture pattern from a distributed hydrologic model, Thales (Grayson *et al.*, 1992) (~140-m^2 grid size) with the field measurements using Time Domain Reflectometry (TDR) (500 points on ~10 m × 20 m grids) at the Tarrawarra watershed (0.105 km^2) in Australia. Using field survey soil map as input, the simulated soil moisture patterns compared well during dry and wet periods, but were problematic during transition periods in spring and fall. Peters-Lidard *et al.* (2001) compared the 5-cm soil moisture pattern predicted by a TOPMODEL based land-atmosphere transfer scheme (TOPLATS-GIS; 30-m resolution) with the soil moisture map derived from the airborne Electrically Steered Thinned Array Radiometer (ESTAR) (200-m resolution) at the Little Washita watershed (530 km^2). The soil map and properties were

*Correspondence to: Yuning Shi, Department of Ecosystem Science and Management, The Pennsylvania State University, 206 Forest Resources Building, University Park, PA 16802, USA.
E-mail: yshi@psu.edu

obtained from a site-specific comprehensive soil property database (Mohanty *et al.*, 2002). The model represented the remotely sensed spatial pattern of soil moisture reasonably well. Rigon *et al.* (2006) and Gebremichael *et al.* (2009) used the ESTAR observations (800-m resolution) at the Little Washita watershed to evaluate a distributed hydrologic model, GEOtop, with 200-m grid resolution with the same comprehensive soil database (Mohanty *et al.*, 2002). The results showed that the drainage network pattern was pronounced in ESTAR soil moisture observations following a storm event, but was totally missed in the GEOtop simulations. Bertoldi *et al.* (2014) compared the GEOtop predicted soil moisture pattern (200-m resolution) with ground surveys and satellite synthetic aperture radar images (~200-m resolution) at the Matsch/Mazia valley watershed (98 km^2) in Italy. A soil map based on local soil survey was used, but the number of soil classes was purposely decreased to avoid over-parameterization. They found that the model simulations show poor capability in reproducing the observed soil moisture spatial variability, with low coefficient of determination (R^2 ~ 0.2) and high errors (RMSE ~ 0.13 $m^3 m^{-3}$). Those studies demonstrated that using hydrologic models to capture the spatial variability of soil moisture at high spatial resolution is challenging, especially when used without a comprehensive and accurate soil map (e.g. Bertoldi *et al.*, 2014).

Determining what data and modelling techniques are required to simulate high-resolution soil moisture patterns will provide important guidance for future hydrologic model applications and model development. Previous studies found that observed watershed-scale soil moisture patterns are primarily controlled by soil texture and topography (Hawley *et al.*, 1983; Burt and Butcher, 1985; Jackson *et al.*, 1995; Nyberg, 1996; Crave and Gascuel-Odoux, 1997; Fitzjohn *et al.*, 1998; Cantón *et al.*, 2004; Western *et al.*, 2004; Takagi and Lin, 2012) and are affected by vegetation in arid or semiarid areas (Seghieri *et al.*, 1997; Gómez-Plaza *et al.*, 2001; Cantón *et al.*, 2004). However, it is very difficult to rank the relative importance of the controlling factors, because those controlling factors interact in a complex manner. Physically based spatially distributed hydrologic models can be used to study the impact of the controlling factors of soil moisture patterns and provide insights into the relative importance of the controlling factors.

This study aims to answer the following questions: (1) Can we predict the observed high-resolution soil moisture pattern (~10 m) using a physically based spatially distributed hydrologic model? (2) What data are needed to resolve fine-scale land surface heterogeneities such as soil moisture patterns using numerical models? and (3) Is the most detailed existing national land cover and soils database sufficient for high-resolution soil hydrologic modelling? We use a coupled land surface hydrologic model, Flux-PIHM (Shi *et al.*, 2013), to provide reasonable answers to these questions. Flux-PIHM couples the Penn State Integrated Hydrologic Model (PIHM) (Qu, 2004; Qu and Duffy, 2007; Kumar, 2009) with the land surface scheme adapted from the Noah land surface model (LSM) (Chen and Dudhia, 2001; Ek *et al.*, 2003). Flux-PIHM adds the ability to simulate the surface energy balance (SEB) and soil moisture profile to PIHM. The model is implemented in the first-order Shale Hills watershed (0.08 km^2) in central Pennsylvania, one watershed within the Susquehanna-Shale Hills Critical Zone Observatory (SSHCZO). The extensive field survey and broad array of observations at this CZO, including spatially distributed soil moisture monitoring sites, make it an ideal site for this study.

MODEL AND DATA

Flux-PIHM

Flux-PIHM incorporates a land-surface scheme into the Penn State Integrated Hydrologic Model (PIHM), a fully coupled, physically based, and spatially distributed hydrologic model. The land surface and hydrologic components are coupled by exchanging water table depth, infiltration rate, recharge rate, net precipitation rate, and evapotranspiration rate between the two model components at every time step. Flux-PIHM simulates surface energy balance, infiltration, recharge, overland flow, groundwater flow, and channel flow at each model grid in a coupled scheme. The model domain is decomposed into unstructured triangular elements and rivers are represented by rectangular elements. Channel flow and overland flow are governed by the 1-D (channel flow) and 2-D (overland flow) St. Venant equations (Saint-Venant, 1871). Unsaturated flow and groundwater flow (with dynamic coupling to the unsaturated zone across water table) are described using the Richards equation, and the unsaturated hydraulic conductivities are calculated using the van Genuchten (1980) equations. Unsaturated water is restricted to vertical transport in the unsaturated zone. In the saturated zone, groundwater flow is horizontal with dynamic coupling to the unsaturated zone across the free surface (water table). The land surface scheme integrates the Penman potential evaporation scheme of Mahrt and Ek (1984), the multiple-layer soil model of Mahrt and Pan (1984), the canopy model of Pan and Mahrt (1987), and the canopy resistance approach of Noilhan and Planton (1989) and Jacquemin and Noilhan (1990). Detailed descriptions and formulations of PIHM and Flux-PIHM are provided by Qu (2004), Qu and Duffy (2007), and Shi *et al.* (2013; 2014).

In this study, we expand the number of standard soil layers in Flux-PIHM from four to ten. The node depths z_i(m) are defined similarly to the Community Land Model Version 3 (CLM3) soil layer definitions (Lawrence *et al.*, 2008):

$$z_i = 0.65\{\exp[0.15(i-0.5)]-1\}, \quad (1)$$

and the thickness of each layer is:

$$\Delta z_i = \begin{cases} 0.5(z_1+z_2), & i=1 \\ 0.5(z_{i+1}-z_{i-1}), & i=2,3,\ldots,N-1, \\ z_N - z_{N-1}, & i=N, \end{cases} \quad (2)$$

where $N=10$ is the number of standard soil layers. Generally, the thicknesses of soil layers increase from 0.11 m for the first layer to 0.38 m for the tenth layer, and the total depth of the standard soil layers is 2.24 m. If the bedrock depth is less than 2.24 m, the number of soil layers is reduced, and the thickness of the lowest layer is adapted to match the depth to bedrock. If the bedrock depth is larger than 2.24 m, one additional soil layer is added as needed.

Study site and data

The Shale Hills watershed is a small-scale, forested, and V-shaped first-order watershed with an area of 0.08 km^2 in central Pennsylvania (Figure 1). This watershed is part of the Susquehanna Shale Hills Critical Zone Observatory (SSHCZO). The mean annual temperature is 10 °C, and the mean annual precipitation is 107 cm. The broad array of observations and extended field surveys and campaigns provide important model input data, calibration data, and evaluation data for this study.

The surface terrain of the Shale Hills catchment is described using airborne light detection and ranging (lidar) data with 1-m horizontal resolution and 2–4 cm accuracy (http://pihm.ics.psu.edu/CZO_NOSL/Lidar.aspx) (Figure 1). The watershed is characterized by relatively steep slopes and narrow ridges. The slopes are interrupted by seven swales (topographic depressional areas). The surface elevation varies from 256 m above sea level at the watershed outlet to 310 m above sea level at the ridge top.

A field survey conducted in 2003 measured the depth to bedrock using augers, and identified five soil series in the watershed (Lin *et al.*, 2006). Figure 2 shows the depth to bedrock map and the soil map obtained from the field campaign. The Weikert soil covers most of the watershed, especially the planar slope and ridge top, and has relative shallow bedrock depth. The Rushtown soil series is found in the centres of the swales, and the Berks soil series appears in between the planar slopes and the swales. The valley floor is covered by the Ernest and Blairton (the latter only found at the head at the stream) soils. Those soil series near the swales and the stream have relatively deep bedrock depths. Lin *et al.* (2006) and Baldwin (2011) measured and derived the soil properties of the five soil series, including the vertical saturated hydraulic conductivity, the horizontal saturated hydraulic conductivity, the soil porosity, and the van Genuchten soil parameters (Table I).

A field survey of all trees over 18-cm diameter at breast height (DBH) was conducted in 2008, which provided a vegetation map of the watershed (Eissenstat *et al.*, 2013).

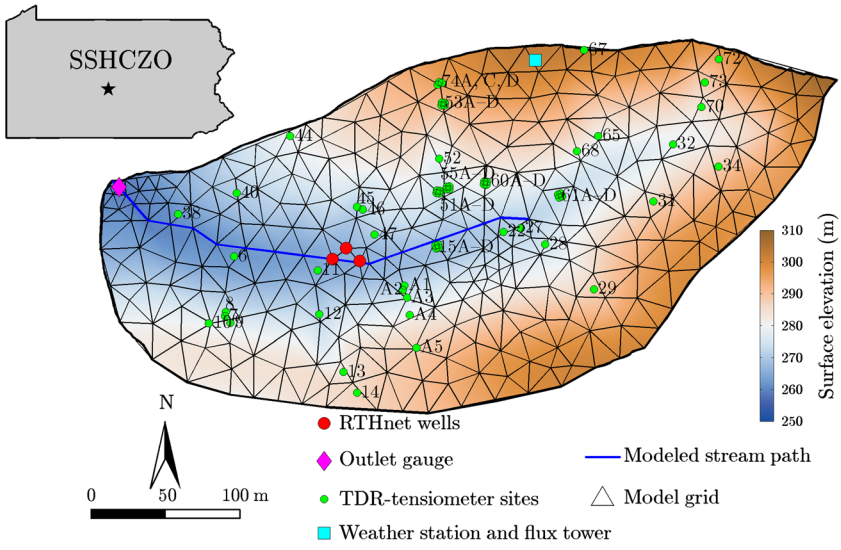

Figure 1. Map of the Shale Hills watershed located in central Pennsylvania and the grids used in Flux-PIHM simulations. The locations of the RTHnet measurements and TDR-tensiometers (with site ID numbers) are shown

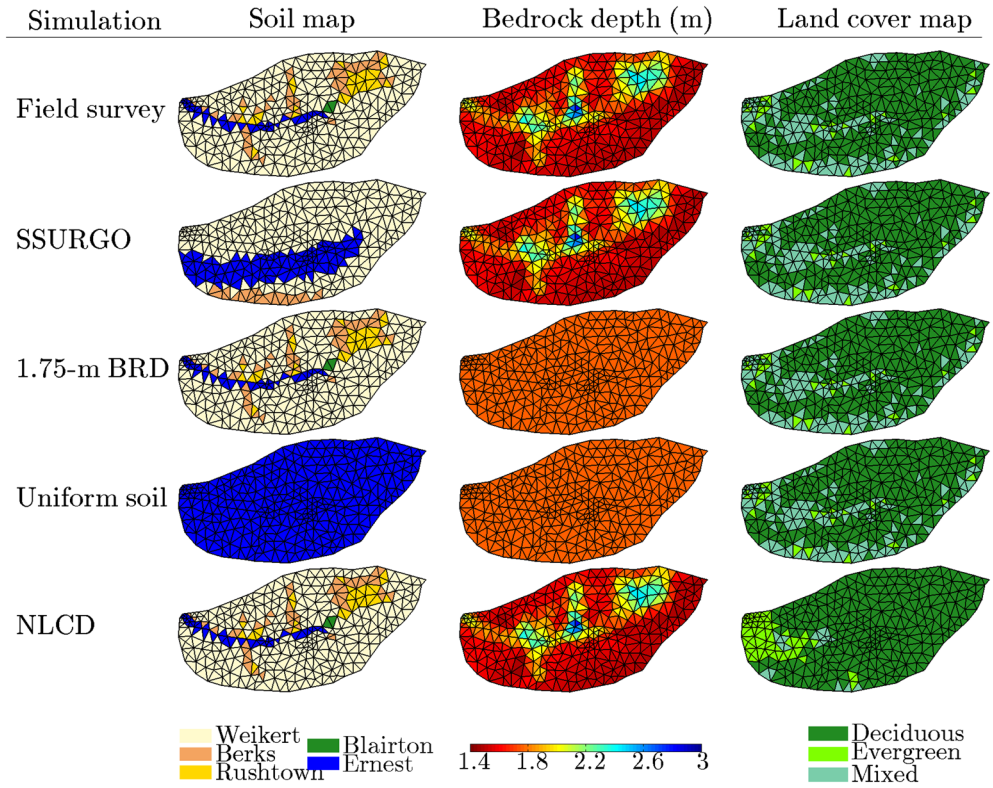

Figure 2. Input maps of soil type, bedrock depth (BRD), and vegetation cover used for different simulations in this study. Field surveys are compared to SSURGO soil type, an assumption of uniform soil type and uniform bedrock depth, and vegetation cover from the National Land Cover Database (NLCD). Note that the 'field survey' BRD map shown in this figure is the observed bedrock depth plus an additional 1.25-m weathered rock layer

Table I. Input soil hydraulic parameters for the simulation with field survey inputs and the SSURGO simulation for each of the five soil series in the Shale Hills watershed, including vertical saturated hydraulic conductivity of infiltration layer (K_{infV}), vertical (K_V) and horizontal (K_H) saturated hydraulic conductivities, porosity (Θ_s), and van Genuchten soil parameters (α and β)

	Weikert		Berks		Rushtown		Blairton		Ernest	
Parameter	Field survey	SSURGO	Field survey	SSURGO	Field survey	SSURGO	Field survey	SSURGO	Field survey	SSURGO
K_{infV} (m d^{-1})	7.86	0.224	13.10	0.255	8.50	—	1.30	—	7.15	0.673
K_V (m d^{-1})	1.40	0.289	1.61	0.250	0.938	—	0.584	—	3.20	0.475
K_H (m d^{-1})	1.04	2.89	0.847	2.50	1.96	—	2.63	—	6.02	4.75
Θ_s (m^3 m^{-3})	0.370	0.471	0.403	0.472	0.425	—	0.418	—	0.493	0.463
α (m^{-1})	8.80	2.46	6.45	2.51	6.50	—	5.34	—	5.82	3.27
β (—)	1.24	1.20	1.21	1.21	1.26	—	1.26	—	1.22	1.32

The sloping areas and ridges of the watershed are covered by several deciduous species. The valley floor and north-facing ridge top are covered by some evergreen species (Wubbels, 2010). Vegetation parameters for different land cover types [e.g. minimum stomatal resistance, albedo, emissivity, roughness length, see Shi *et al.* (2013) for details] are obtained from the modified International Geosphere–Biosphere Programme (IGBP) Moderate Resolution Imaging Spectroradiometer (MODIS) 20-category vegetation (land use) data (http://www.ral.ucar.edu/research/land/technology/ lsm/parameters/).

To test the adequacy of the national scale database for high-resolution hydrologic modelling, data from the Soil Survey Geographic Database (SSURGO) and the National Land Cover Database (NLCD) are used for comparison in this study. Figure 2 shows the SSURGO soil map and NLCD land cover map for the Shale Hills watershed. Because of the limitation of its spatial resolution (30 m), SSURGO soil map cannot resolve the soil types around the swales. In addition, the location of the Ernest soil series in the SSURGO soil map deviates from the local soil survey (Figure 2). The *a priori* soil hydraulic

properties for SSURGO soil series are obtained by applying pedotransfer functions (PTF) (Wösten *et al.*, 2001, their Table II) to textural classes in SSURGO, and are shown in Table I. The NLCD land cover map captures the deciduous trees on the slopes and the evergreen trees on the valley floor near the outlet, but misses the evergreen trees on the north-facing ridge top (Figure 2). The vegetation parameters for the NLCD land cover types are obtained from the modified IGBP MODIS 20-category vegetation (land use) data.

The forcing data used in this study are the same as those used in Shi *et al.* (2013). Precipitation, air temperature, and relative humidity data are obtained from the real time hydrologic monitoring network (RTHnet) weather station at the SSHCZO. Downward longwave radiation and downward solar radiation are obtained from the Surface Radiation Budget Network (SURFRAD) (Augustine *et al.*, 2000) Penn State University station near the Shale Hills watershed. Surface air pressure and wind speed data are obtained from the Penn State SURFRAD station (prior to April 2009) and the SSHCZO eddy-covariance tower (after April 2009). Given the small scale (0.08 km^2) of the watershed, spatially uniform meteorological forcing is used for this study. The MODIS 8-day composite leaf area index (LAI) data (Knyazikhin *et al.*, 1999; Myneni *et al.*, 2002) are rescaled based on the comparison between the MODIS product and CZO field measurements (Naithani *et al.*, 2013) to represent the vegetation phenology (Shi *et al.*, 2013). MODIS LAI has a spatial resolution of 1 km^2 thus cannot resolve spatial structure in LAI within the watershed.

Calibration data include stream discharge, and point measurements of groundwater level and soil moisture. Stream discharge is measured with a V-notch weir at the outlet of watershed. The water level at the weir is measured with a Campbell CS420-L pressure transducer and then converted to discharge rate using a rating curve developed by Nutter (1964). The groundwater level and soil moisture data used for calibration are collected from three RTHnet wells drilled near the stream. The water table depth (WTD; distance from the land surface to the groundwater table) measurements (using Campbell CS420-L pressure transducers) collected in different wells are averaged to represent the mean WTD observed within the single Flux-PIHM grid that includes the RTHnet wells. The multiple volumetric soil moisture content observations (using Decagon Echo2 EC-20 soil moisture sensors) are collected at 10, 30, and 50-cm depths. Measurements from those three wells are averaged to represent the observed top 50-cm soil water content (SWC). The model domain is discretized such that the three RTHnet wells are located at three vertices of one model grid (Figure 1). The point measurements of WTD and SWC are used to optimize the model predictions of WTD and SWC in that model grid that represents the RTHnet wells. More details about the forcing and calibration data can be found in Shi *et al.* (2013).

Soil moisture measurements were collected across the watershed at a weekly to biweekly interval with a handheld TRIME-FM (IMKO, Germany) TDR probe on 15 days from 26 April to 09 October 2009. Volumetric soil moisture measurements were collected at 10, 20, 40, 60, 80, and 100-cm depths by inserting the TDR probe into Schedule 40 PVC access tubes that were buried at 61 sites across the watershed. Data collection on each day typically took 6–8 h, from around 0800 LST to around 1600 LST. Holes were drilled down to 110 cm or bedrock at each site to install the access tubes. Because many of the sites have shallow depth to bedrock (as shallow as $<$20 cm), not all sites have measurements below 10 cm. Therefore, only the measurements at 10-cm depth are used for this study.

A geostatistical technique called kriging with an external drift (Diggle and Ribeiro, 2007) is used at each TDR site to calculate continuous catchment-wide fields of 10-cm soil moisture for each measurement date in 2009 to help illustrate the observed soil moisture patterns. Kriging with an external drift is a form of kriging where auxiliary variables are used in a linear regression model to estimate

Table II. Statistical analysis of hourly model predictions of discharge (Q), water table depth (WTD), and top 50-cm soil water content (SWC) from 1 Apr to 1 Nov 2009, including the Nash–Sutcliffe coefficient (NSE) for Q, and the correlation coefficient (R), and the root mean square error (RMSE) for WTD and SWC

	Q	WTD		SWC	
Simulation	NSE	R (—)	RMSE (m)	R (—)	RMSE ($m^3\,m^{-3}$)
Field survey	0.778	0.836	0.168	0.743	0.021
SSURGO	0.782	0.820	0.179	0.784	0.024
1.75-m BRD	0.770	0.759	0.221	0.725	0.026
Uniform soil	0.902	0.803	0.186	0.776	0.018
NLCD	0.788	0.843	0.164	0.731	0.021

the local means of a predicted variable, and then ordinary kriging is performed on the model residuals to interpolate them across space. We use topographic variables derived from the lidar topography data as auxiliary variables, and a stepwise regression procedure (Venables and Ripley, 2002) is used to define the regression equation, where the regression equation with the lowest Akaike's Information Criterion is chosen. An exponential spatial model was used to estimate the spatial autocorrelation structure of model residuals. The R package GeoR (Diggle and Ribeiro, 2007) is used to conduct the soil moisture kriging.

FLUX-PIHM SETUP

The Shale Hills watershed model domain is decomposed into 535 triangular grids with an average grid size of 157 m^2. The stream channel is represented by 20 stream segments. The model grid configurations are presented in Figure 1.

To identify the controlling factors of the observed soil moisture patterns in Flux-PIHM, we examine five different combinations of soil maps, land cover maps, and bedrock depth maps (Figure 2). In the 'field survey' simulation, the surface topography map obtained from the 1-m lidar data, the depth to bedrock map and soil map obtained from the field campaign, and the land cover map obtained from the tree survey are projected to the model grids to define the surface elevation, bedrock depth, vegetation type, and soil type of each model grid. An extra 1.25 m is added to the measured bedrock depths for all model grids to account for flow through a deeper weathered shale layer (Shi *et al.*, 2013). Driven by field survey inputs, this simulation represents our best effort to numerically replicate the watershed, and is used to evaluate the model's ability of reproducing the observed soil moisture spatial patterns.

The '1.75-m BRD' simulation uses the same soil map and soil parameters as the field survey simulation, but has a uniform bedrock depth of 1.75 m, which is the average bedrock depth in the field survey simulation. In the 'uniform soil' simulation, all model grids have the same soil type (Ernest) and bedrock depth (1.75 m). The 'SSURGO' simulation uses the SSURGO soil map, the soil properties calculated using the pedotransfer functions (Wösten *et al.*, 2001), and the same bedrock depth map as in the field survey simulation. The 'NLCD' simulation uses the same soil map, soil parameters, and bedrock depths as the field survey simulation, but uses the NLCD land cover map instead of the field survey vegetation cover map. Results from these simulations are compared with the simulation driven by field survey inputs to identify the controlling factors of the soil moisture pattern, and to test whether the national database is sufficient in high-resolution hydrologic modelling.

All simulations start from 0000 UTC 1 January 2008, with a model time step of 1 min and an output interval of 1 h. All simulations are separately manually calibrated using outlet discharge, RTHnet water table depth, and RTHnet top 50-cm soil water content measurements to make sure they can all reproduce the watershed-scale (i.e. discharge) and point (soil water content and water table depth) observations. The hydrologic parameters that show relatively strong identifiability in the model sensitivity analysis (Shi *et al.*, 2014) are calibrated, including the vertical saturated hydraulic conductivity of infiltration layer, vertical and horizontal saturated hydraulic conductivities, soil porosity, van Genuchten soil parameters, and vertical and horizontal macropore hydraulic conductivities. The other parameters are kept the same among all simulations. For details about those parameters, please see Shi *et al.* (2013; 2014).

The thicknesses of the top two soil layers in Flux-PIHM are 10.7 cm and 12.3 cm, respectively. For this assessment, the simulated soil moisture content from the top two layers are averaged to be compared with the measurements at the 10-cm depth:

$$\overline{\Theta^m} = \frac{\Theta_1^m \Delta z_1 + \Theta_2^m \Delta z_2}{\Delta z_1 + \Delta z_2}, \tag{3}$$

where $\overline{\Theta^m}$ is the simulated 10-cm soil moisture for a model grid, Θ_i^m is the simulated volumetric soil water content at the i^{th} model layer, and Δz_i is the thickness of the i^{th} model layer, following Equation 2. For each measurement day, Flux-PIHM predictions between 0800 LST and 1600 LST (corresponding to the field data collection time) are averaged to represent the predicted soil moisture pattern of the measurement day. The simulated spatial patterns in soil moisture for all measurement days in 2009 are compared with observations for each set of input data. The model-data comparisons for various input data sets are used to evaluate the importance of site-specific input data for accurate simulation of the high-resolution spatial pattern in soil moisture.

RESULTS

Predictions of discharge and point measurements

Figure 3 and Table II present the comparison of hourly discharge, water table depth (WTD), and top 50-cm soil water content (SWC) between RTHnet observations and different Flux-PIHM simulations, as well as the statistical analysis of these results. Although our different simulations use different soil maps, bedrock depths, and land cover maps, they provide similar performance in terms of

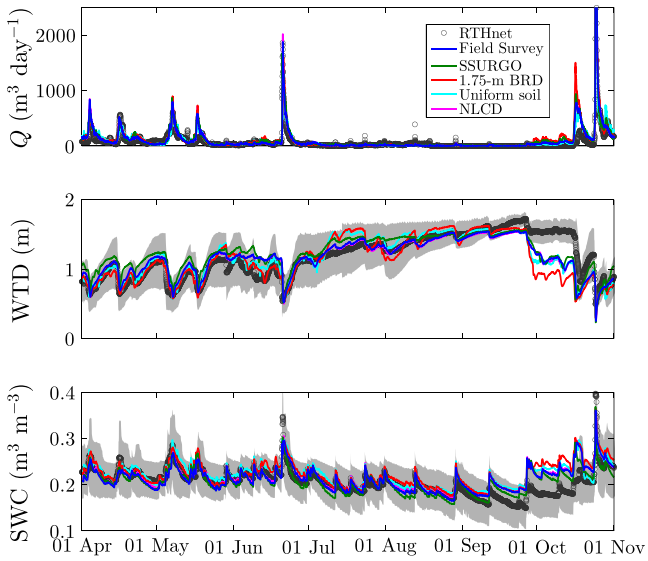

Figure 3. Comparison of watershed outlet discharge (top), water table depth (middle), and top 50-cm soil water content (bottom) between observations and the suite of Flux-PIHM simulations from 1 Apr to 1 Nov 2009. The WTD and SWC observations are averages among three wells. Circles are observations, and the shaded areas show the representativity errors in WTD and SWC, quantified by the standard deviation of the three RTHnet measurements

the predictions of outlet discharge, as well as predictions of WTD and SWC at the RTHnet wells after calibration. All simulations have the ability to reproduce the observed discharge and point measurements of WTD and SWC after calibration (Figure 3 and Table II). The Nash–Sutcliffe model efficiency coefficients (NSEs) (Nash and Sutcliffe, 1970) for discharge predictions range from 0.770 and 0.902 across the different simulations. The root mean square errors (RMSEs) of WTD predictions are all lower than 0.23 m, and the correlation coefficients (R) are all higher than 0.75. As for the SWC predictions, the RMSEs are lower than $0.026\,m^3\,m^{-3}$, and the correlation coefficients are all higher than 0.72.

Observed soil moisture pattern at the Shale Hills watershed

Figure 4 presents the observed 10-cm soil moisture pattern at the Shale Hills watershed for 15 days in 2009. Generally, the observation points near the stream and in the swales are wetter than the points on the planar slopes. The watershed soil moisture pattern shows considerable spatial heterogeneity. For example, Sites A1, A2, and A3 are within 10 m to each other (for locations of these sites, see Figure 1). The soil moisture conditions, however, are significantly different. On most of the measurement days, the 10-cm soil moisture observed at the A3 site is about $0.1\,m^3\,m^{-3}$ lower than the other two sites. As for the temporal variation, the watershed is wetter in April, May, and October, but drier in August and September when the swale characteristics become less prominent.

Prediction of soil moisture pattern from the simulation using field survey inputs

Figure 5 presents the Flux-PIHM prediction of soil moisture content at 10-cm depth using the field survey input. Note that the simulated soil moisture patterns presented in Figure 5 show the predictions from the triangular grids in the model, but do not include the river segments, which are assumed to be saturated at all times. Flux-PIHM predicts wetter soil near the stream and in the swales, and drier soil on the planar slope. The model simulation, however, shows notable dry bias on most of the days. This is probably because the model is only calibrated using soil moisture observations at one point. The model simulated soil moisture patterns are much smoother than the observations.

Figure 6a compares the simulated and observed 10-cm soil moisture for each TDR site. If there are multiple TDR sites in one Flux-PIHM model grid, the measurements within the same grid are averaged. Similar to Figure 5, Figure 6a demonstrates that the simulation using the field survey inputs systematically underestimates the 10-cm soil moisture, especially in the wetter areas. The mean bias is larger when the watershed is wetter (from April to July and in October) and smaller when the watershed is dryer (in August and September). The RMSEs range from 0.034 to $0.092\,m^3\,m^{-3}$ on different days. Despite the notable dry bias in the prediction, the spatial correlations are always larger than 0.5, except for 3 October, which demonstrates the ability of the Flux-PIHM model to simulate the macro watershed soil moisture patterns. Flux-PIHM is able to predict the relative wetness of the

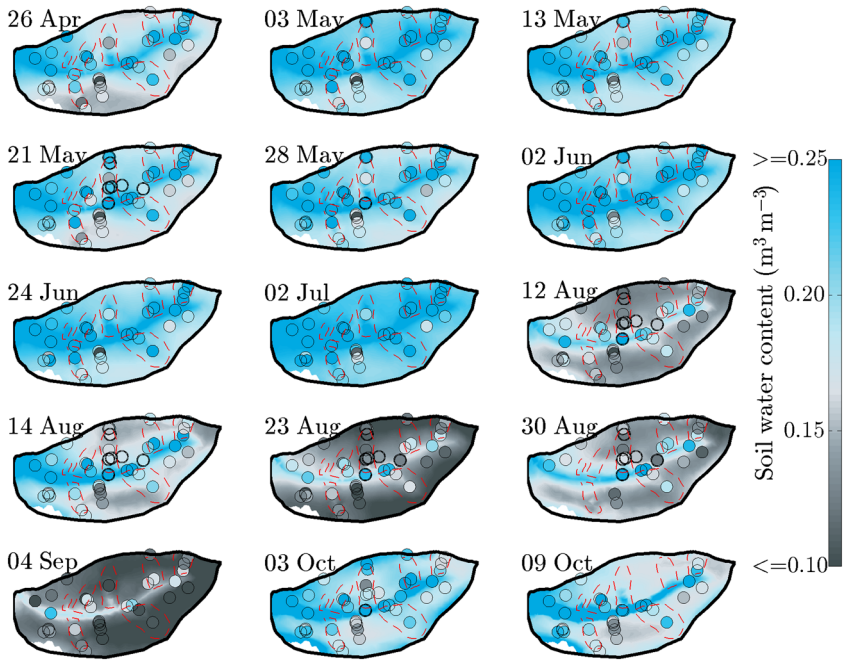

Figure 4. Observed soil moisture patterns at 10-cm depth of the Shale Hills watershed for 15 days in 2009. The coloured dots represent the TDR point measurements, and the background is the soil moisture distribution obtained using regression kriging

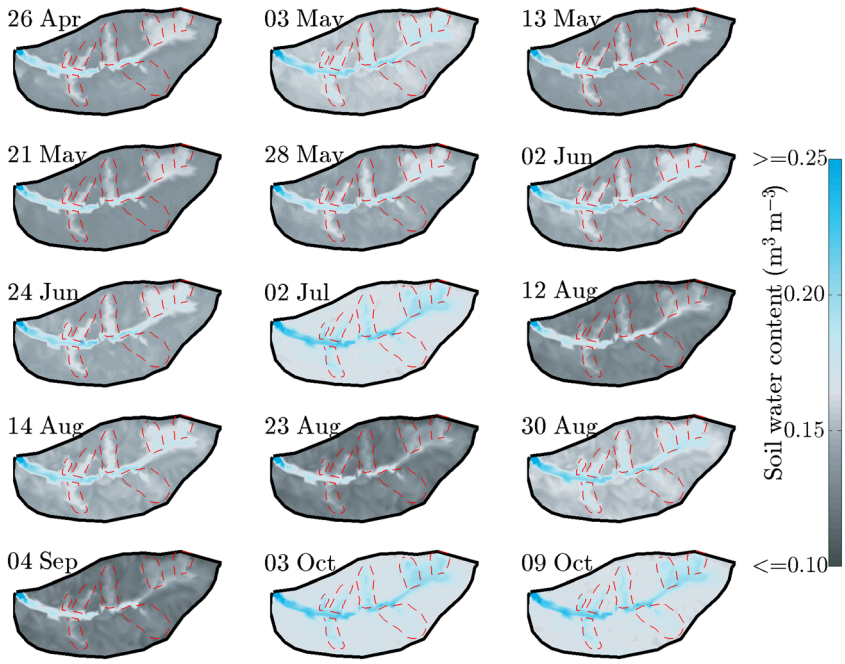

Figure 5. Flux-PIHM simulated soil moisture (at 10-cm depth) spatial patterns from the field survey simulation for 15 days in 2009

soil types, for example the Ernest soil type is always wetter than the Weikert soil type. But it is clear that the observations show greater variability in soil moisture within a soil type than the simulation. The primary source of spatial variability in soil moisture in the model appears to be soil type.

Figure 6b shows the temporal variation of the observed and predicted average soil moisture at the TDR sites for the measurement days. The model is able to capture the general day-to-day variation in soil moisture, but has a notable dry bias and underestimates the magnitude of the temporal variation.

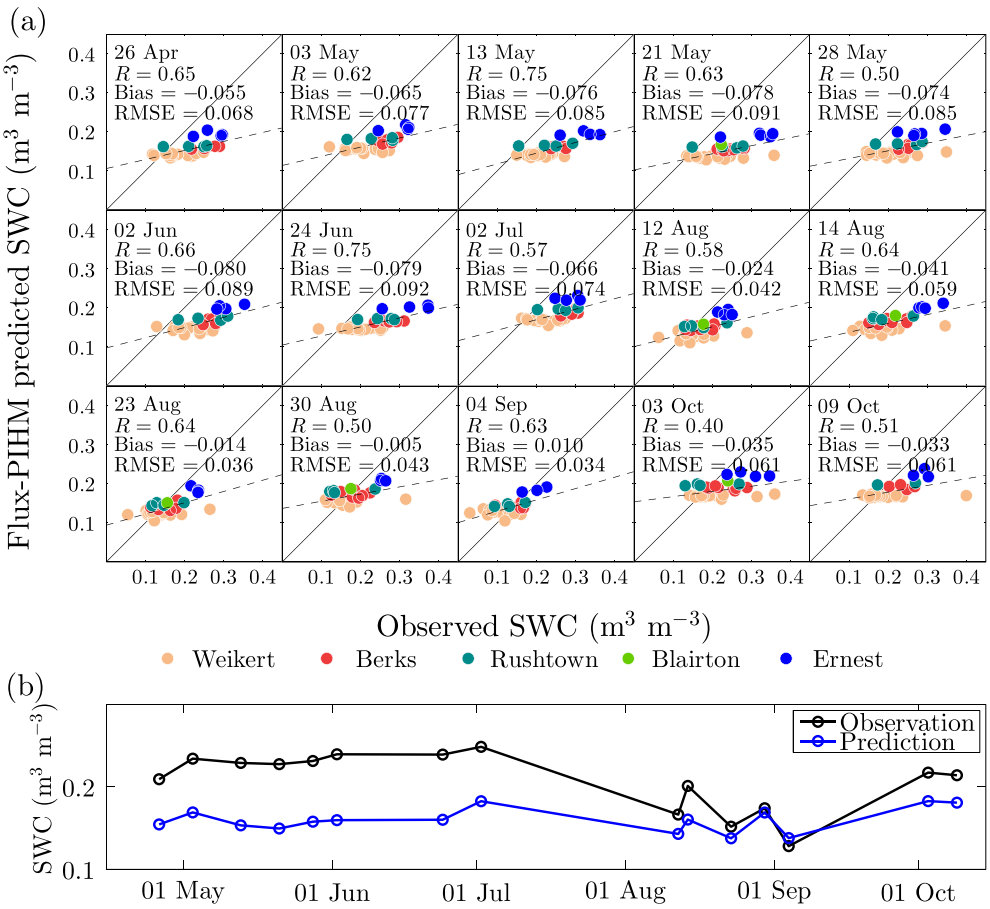

Figure 6. (a) TDR observations versus Flux-PIHM simulation using field survey input data for 10-cm soil moisture at each TDR site. Correlation coefficients and RMSEs are also shown. The solid black lines are the 1:1 lines, and the dashed black lines represent linear fits. Different colours represent different soil types in Flux-PIHM. The unit for bias and RMSE is m^3 m^{-3}. (b) Temporal variations of observed and simulated soil moisture (spatial average)

Comparison of the soil moisture pattern across different simulations

To identify and compare the relative importance of the controlling factors of the soil moisture pattern, we compare the soil moisture patterns predicted by different simulations. The results are similar across all days. For the sake of brevity we focus on the temporal average of soil moisture patterns across all 15 measurement days. The predicted soil moisture patterns from different simulations averaged across all measurement days are presented in Figure 7, and the predicted *versus* observed one-to-one comparisons are presented in Figure 8.

The pattern of soil moisture predicted by the SSURGO simulation (Figure 7b) strongly correlates with the pattern of the SSURGO soil map (Figure 2), but differs from the observed soil moisture pattern. The spatial correlation between the SSURGO simulation and point measurements is −0.02 (Figure 8b). The SSURGO simulation is characterized by a broad dry soil area on the southern slope (Figure 7b), corresponding to the location of the Ernest soil series in the SSURGO soil map (Figure 2). The simulation using field survey inputs predicts that the Ernest soil series is always wetter than the Weikert soil series, the opposite of the SSURGO simulation. This is caused by the different soil hydraulic parameters in the field survey simulation and the SSURGO simulation (Table I). To test this, we perform another simulation, which uses the SSURGO soil map with the soil parameters from the field survey. The soil moisture pattern predicted in this simulation (results not shown here) still correlates with the SSURGO soil map, except that the Ernest soil series is wetter than the Weikert soil series, as predicted in the simulation using field survey inputs.

The 1.75-m BRD simulation (Figure 7c) generally captures the overall observed soil moisture pattern, predicting wetter soil near the stream and in the swales, and dryer soil on the planar slope. This simulation, however, predicts stronger contrast between wet and dry soils, and has a larger spatial variability compared to the simulation with field survey inputs. The soil moisture

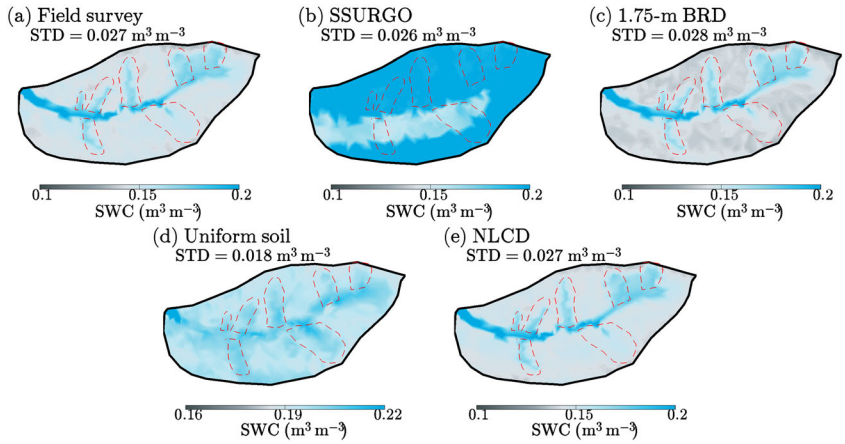

Figure 7. Comparison of 10-cm soil moisture spatial patterns averaged across all measurement days from simulations using different input data sets (Figure 2). The spatial standard deviations are presented to quantify the predicted spatial variability of soil moisture

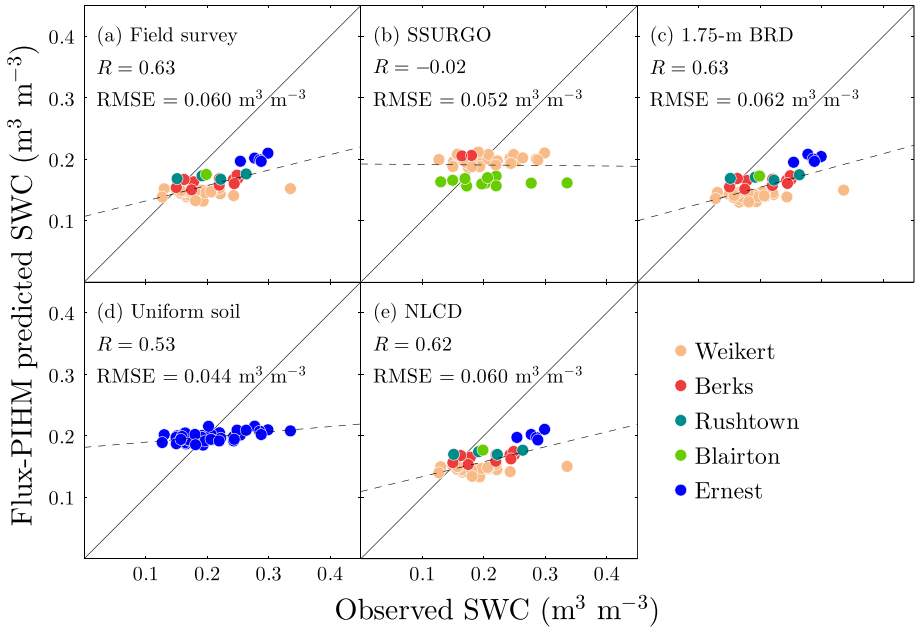

Figure 8. TDR point observations versus simulated 10-cm soil moisture using different input data sets (Figure 2). Each dot represents the observations or predictions at one TDR site averaged over all measurement days. Different colours represent different soil types in Flux-PIHM

near the stream (the Ernest soil series) is almost the same as in the simulation with field survey inputs, but the soil moisture on the planar slope is lower than in the field survey simulation. Generally, our simulations show that increasing the bedrock depth in the model tends to decrease the surface soil moisture. Compared with the simulation with field survey inputs, the 1.75-m BRD simulation has shallower bedrock depths near the stream but deeper bedrock depths on the planar slope (Figure 2), which leads to wetter soil near the stream and dryer soil on the planar slope. Because we calibrate all model simulations such that the soil moisture near the stream matches the observation, the combined result is that the soil moisture near the stream is almost the same as in the simulation with field survey inputs, but the soil moisture on the planar slope is much dryer.

The uniform soil simulation (Figure 7d) significantly underestimates the variability in soil moisture, but does predict relatively wetter soil near the stream and in the swales. The spatial correlation between this simulation and the measurements is 0.53. The predicted spatial standard deviation of soil moisture is about 67% of that in the simulation with field survey inputs. Because the soil and bedrock depth is uniform in this simulation, the predicted spatial pattern is mainly caused by lateral groundwater flow, driven by surface topography.

The soil moisture pattern predicted by the NLCD simulation (Figure 7e) is almost identical to the simulation with field survey inputs, which indicates that the relatively small differences in vegetation distribution between the NLCD database and our site survey are not a controlling factor of the observed soil moisture pattern at the Shale Hills watershed. It is also important to note that our simulation does not take into account differences across tree species, or spatial gradients in leaf area index (e.g. Naithani *et al.*, 2013).

DISCUSSION AND CONCLUSIONS

The results from these model simulations based on field survey input data show that Flux-PIHM, a physically based spatially distributed land surface hydrologic model, can reasonably reproduce the observed macro soil moisture pattern in the Shale Hills watershed. The average spatial correlation is 0.63 and the average RMSE is $0.06\,m^3\,m^{-3}$. Calibrated using only watershed-scale measurements (i.e. discharge) and point measurements (i.e. soil moisture and water table depth at one location), and driven by spatially uniform forcing data, Flux-PIHM is able to resolve the observed hillslope scale (10^1 m) soil moisture pattern across the watershed and reproduce the day-to-day variation of soil moisture.

Bertoldi *et al.* (2014) and Western *et al.* (1999) both found that the hydrologic model predicted soil moisture patterns tend to cluster with respect to the input soil types, which is also shown in our study (Figures 5 and 6). It is clear from comparisons at observation points that the simulation underestimates variability in soil moisture within soil types (Figure 6). In Flux-PIHM, all grids that have the same soil series/landcover types use the same soil hydraulic/landcover properties. We cannot conclude from the data available if this weakness in the simulations is because of mixed soils and vegetation types that are not represented in our input data, or processes such as lateral flow that are not being simulated properly. A study of the variation in soil properties within soil types might clarify the source of this discrepancy.

Most of the previous studies investigated the controlling factors of soil moisture patterns by examining the relationship between topography, soil properties, land cover, and soil moisture using statistical analysis (e.g. Hawley *et al.*, 1983; Jackson *et al.*, 1995; Nyberg, 1996; Crave and Gascuel-Odoux, 1997; Fitzjohn *et al.*, 1998; Cantón *et al.*, 2004). This study provides an alternative means to explore the influences on soil moisture patterns using a numerical model. The simulations that vary input data sets show strong modelling evidence that the soil distribution and soil hydraulic parameters have the dominant effect on predicted spatial pattern in soil moisture at the Shale Hills watershed. The surface topography and depth to bedrock also affect the soil moisture pattern in this watershed. The relatively small variation in vegetation distribution tested has negligible effects on the soil moisture pattern. Baldwin *et al.* (submitted) calculated the temporal autocorrelation of soil moisture (2007–2010) from the 61 sites across Shale Hills. They found that the combination of topography and a digital soil map was significantly more accurate in characterizing watershed-scale soil moisture variation than five other prevailing stratification systems, which indicates that the soil moisture pattern at the Shale Hills watershed is controlled by topography and soil types; our model results agree with their findings.

In all simulations, the predicted soil moisture patterns strongly correlate with the input soil maps. The relative magnitude of soil hydraulic parameters of different soil types appears to determine the relative wetness of soil types. For example, in the SSURGO simulation, the model predicts that the Ernest soil series is drier than the Weikert soil series when SSURGO parameters are used, but predicts the opposite when the field survey parameters are used. Flux-PIHM uses the single global calibration multiplier method (Pokhrel and Gupta, 2010; Wallner *et al.*, 2012; Shi *et al.*, 2013) to calibrate model parameters. This method effectively reduces the dimension of parameter space for calibration. By using the global calibration multiplier, the ratios between the *a priori* parameter values of different soil types are preserved. Calibration of this multiplier can improve the predictions at the watershed-scale or at points, but it cannot improve the prediction of relative wetness if the ratios between *a priori* parameters are poorly estimated. The estimate of *a priori* parameters is thus critical to yield reasonable spatial patterns of variable when the global calibration multiplier method is used. Although it is possible to solve for different calibration multipliers for different soil types, this method significantly increases the dimension of space for parameter calibration, and is almost impractical in larger watersheds with large numbers of soil types.

The surface topography also appears to affect the soil moisture pattern. Results from the uniform soil simulation show that the model is able to reflect the impact of topography on soil moisture pattern, owing to the spatially distributed physically based hydrologic component, especially the simulation of horizontal groundwater flow. This demonstrates the potential for Flux-PIHM to be used to study the impact of topography on hydrological, land surface, and biogeochemical processes. The impact of topography on the spatial pattern in soil moisture, however, is relatively small compared to the impact of soil distribution. The depth to bedrock does not affect the general pattern of soil moisture, but has an

effect on the amplitude of the spatial variability in the surface soil moisture, suggesting that accurate bedrock depth data is another important input data set.

For the soil parameters measured and derived by Lin *et al.* (2006) and Baldwin (2011), the Weikert soil series has larger α and β, and smaller Θ_s values than the Ernest series. For the SSURGO simulation, however, the Weikert soil series has smaller α and β, and larger Θ_s values. The Flux-PIHM sensitivity analysis demonstrated that the predicted soil saturation is very sensitive to α and β values (Shi *et al.*, 2014). The wrong relative magnitude of the van Genuchten parameters between two soil series in the SSURGO simulation leads to wrong relative wetness. It suggests that the combination of SSURGO soil map and pedotransfer functions is not adequate for high-resolution soil moisture pattern prediction. However, it is not clear if the error is because of the SSURGO soil properties (e.g. clay, silt, and organic matter percentages, and bulk density), or the pedotransfer functions (PTF) (Wösten *et al.*, 2001) used to estimate the soil hydraulic parameters. Field soil surveys are critical in providing accurate soil map and soil hydraulic parameters for spatially distributed hydrologic simulation.

While the static input data (e.g. soil maps and parameters, landcover maps, and bedrock depth maps) used by the different simulations vary considerably, the discharge predictions and point WTD and SWC predictions from the different simulations are very similar after each is manually calibrated, and all show good agreement with the observations (Figure 3 and Table II). This illustrates the phenomenon of 'equifinality' (Beven, 1993), i.e. acceptable model predictions are achieved using different combinations of model parameters.

Because the simulations are calibrated using integrated top 50-cm soil moisture measurements at one point in addition to discharge and point water table depth measurements, the model produces a notable dry bias using the field survey input. This implies a potential drawback of using point soil moisture measurements for model calibration. Because of the high spatial heterogeneity of soil moisture (Figure 4), calibrating using point measurements cannot guarantee that the model captures the watershed-scale soil moisture conditions. Intermediate scale measurements, e.g. the cosmic-ray soil moisture observing system (COSMOS) (Zreda *et al.*, 2008), may provide better calibration data for model application at small watersheds.

Flux-PIHM reproduces the day-to-day variation of soil moisture, and resolves the observed overall soil moisture pattern when appropriate input data are used. This ability of Flux-PIHM to resolve high-resolution hillslope soil moisture patterns is especially significant for simulations at small watersheds, which represent a large areal fraction of many landscapes. It makes the model a good platform for coupling biogeochemistry models to enable the quantitative investigation of the effects of landscape on biogeochemical processes.

The results highlight the needs to improve the soil database for small scale watershed modelling. Field surveyed soil maps and hydrologic parameters are not commonly available for every watershed. Hydrologic models generally rely on national scale soil database to provide soil maps. Soil hydraulic properties are usually estimated using different approximations because of the lack of reliable soil property database. The most detailed national soils database (SSURGO, 30-m resolution), however, is still insufficient for high-resolution watershed modelling as shown in our study. National scale soils database with higher spatial resolution and higher accuracy soil maps and hydraulic parameters are needed for hydrologic simulations in low-order watersheds.

ACKNOWLEDGEMENTS

This research was supported by the National Science Foundation Susquehanna Shale Hills Critical Zone Observatory project through grant EAR 0725019. Logistical support and relevant data were provided by the NSF-supported Susquehanna Shale Hills Critical Zone Observatory.

REFERENCES

Augustine JA, DeLuisi JJ, Long CN. 2000. SURFRAD—a national surface radiation budget network for atmospheric research. *Bulletin of the American Meteorological Society* **81**: 2341–2357. DOI: 10.1175/1520-0477(2000)081<2341:SANSRB>2.3.CO;2

Baldwin D. 2011. Catchment-scale soil water retention characteristics and delineation of hydropedological functional units in the Shale Hills Catchment. M.S. thesis, Department of Soil Science, The Pennsylvania State University; 126.

Baldwin DC, Naithani KJ, Lin HS. Submitted. Integrated soil-terrain stratification for characterizing catchment-scale soil moisture variation. *Geoderma*.

Bertoldi G, Della Chiesa S, Notarnicola C, Pasolli L, Niedrist G, Tappeiner U. 2014. Estimation of soil moisture patterns in mountain grasslands by means of SAR RADARSAT2 images and hydrological modeling. *Journal of Hydrology* **516**: 245–257. DOI: 10.1016/j.jhydrol.2014.02.018

Beven K. 1993. Prophecy, reality and uncertainty in distributed hydrological modelling. *Advances in Water Resources* **16**(1): 41–51. DOI: 10.1016/0309-1708(93)90028-E

Burt TP, Butcher DP. 1985. Topographic controls of soil moisture distributions. *Journal of Soil Science* **36**: 469–486. DOI: 10.1111/j.1365-2389.1985.tb00351.x

Cantón Y, Solé-Benet A, Domingo F. 2004. Temporal and spatial patterns of soil moisture in semiarid badlands of SE Spain. *Journal of Hydrology* **285**: 199–214. DOI: 10.1016/j.jhydrol.2003.08.018

Chen F, Dudhia J. 2001. Coupling an advanced land surface-hydrology model with the Penn State-NCAR MM5 modeling system. Part I: Model implementation and sensitivity. *Monthly Weather Review* **129**(4): 569–585. DOI: 10.1175/1520-0493(2001)129<0569:CAALSH>2.0.CO;2

Crave A, Gascuel-Odoux C. 1997. The influence of topography on time and space distribution of soil surface water content. *Hydrological Processes* **11**: 203–210. DOI: 10.1002/(SICI)1099-1085(199702)11:2<203::AID-HYP432>3.0.CO;2-K

Diggle PJ, Ribeiro PJ Jr. 2007. *Model Based Geostatistics*. Springer: New York; 228.

Eissenstat D, Wubbles J, Adams T, Osborne J. 2013. Susquehanna Shale Hills Critical Zone Observatory Tree Survey (2008). *Integrated Earth Data Applications (IEDA)*. DOI: 10.1594/IEDA/100268

Ek MB, Mitchell KE, Lin Y, Rogers E, Grummann P, Koren V, Gayno G, Tarpley JD. 2003. Implementation of Noah land surface model advances in the National Centers for Environmental Prediction operational Mesoscale Eta Model. *Journal of Geophysical Research* **108**: 8851. DOI: 10.1029/2002JD003296

Fitzjohn C, Ternan JL, Williams AG. 1998. Soil moisture variability in a semi-arid gully catchment: implications for runoff and erosion control. *Catena* **32**(1): 55–70. DOI: 10.1016/S0341-8162(97)00045-3

Gebremichael M, Rigon R, Bertoldi G, Over TM. 2009. On the scaling characteristics of observed and simulated spatial soil moisture fields. *Nonlinear Processes in Geophysics* **16**: 141–150. DOI: 10.5194/npg-16-141-2009

Gómez-Plaza A, Martınez-Mena M, Albaladejo J, Castillo VM. 2001. Factors regulating spatial distribution of soil water content in small semiarid catchments. *Journal of Hydrology* **253**: 211–226. DOI: 10.1016/S0022-1694(01)00483-8

Grayson RB, Moore ID, McMahon TA. 1992. Physically based hydrologic modeling: 1. A terrain-based model for investigative purposes. *Water Resources Research* **28**(10): 2639–2658. DOI: 10.1029/92WR01258

Hawley, ME, Jackson TJ, McCuen RH. 1983. Surface soil moisture variation on small agricultural watersheds. *Journal of Hydrology* **62**: 179–200. DOI: 10.1016/0022-1694(83)90102-6

Jackson TJ, Le Vine DM, Swift CT, Schmugge TJ, Schiebe FR. 1995. Large area mapping of soil moisture using the ESTAR passive microwave radiometer in Washita'92. *Remote Sensing of Environment* **54**(1): 27–37. DOI: 10.1016/0034-4257(95)00084-E

Jacquemin B, Noilhan J. 1990. Sensitivity study and validation of a land surface parameterization using the HAPEX-MOBILHY data set. *Boundary-Layer Meteorology* **52**(1): 93–134. DOI: 10.1007/BF00123180

Knyazikhin Y, Glassy J, Privette JL, Tian Y, Lotsch A, Zhang Y, Wang Y, Morisette JT, Votava P, Myneni RB, Nemani RR, Running SW. 1999. MODIS leaf area index (LAI) and fraction of photosynthetically active radiation absorbed by vegetation (FPAR) product (MOD15) algorithm theoretical basis document. Theoretical basis document, NASA Goddard Space Flight Center, Greenbelt, Maryland.

Kumar M. 2009. Toward a hydrologic modeling system. Ph.D. thesis, The Pennsylvania State University; 251.

Lawrence DM, Slater AG, Romanovsky VE, Nicolsky DJ. 2008. Sensitivity of a model projection of near-surface permafrost degradation to soil column depth and representation of soil organic matter. *Journal of Geophysical Research* **113**: F02011. DOI: 10.1029/2007JF000883

Liang X, Wood EF, Lettenmaier DP. 1996. Surface soil moisture parameterization of the VIC-2L model: evaluation and modification. *Global and Planetary Change* **13**: 195–206. DOI: 10.1016/0921-8181(95)00046-1

Liang, X, Xie Z, Huang M. 2003. A new parameterization for surface and groundwater interactions and its impact on water budgets with the variable infiltration capacity (VIC) land surface model. *Journal of Geophysical Research* **108**: 8613. DOI: 10.1029/2002JD003090

Livneh B, Restrepo PJ, Lettenmaier DP. 2011. Development of a unified land model for prediction of surface hydrology and land–atmosphere interactions. *Journal of Hydrometeorology* **12**: 1299–1320. DOI: 10.1175/2011JHM1361.1

Lin H-S, Kogelmann W, Walker C, Bruns MA. 2006. Soil moisture patterns in a forested catchment: a hydropedological perspective. *Geoderma* **131**(3): 345–368. DOI: 10.1016/j.geoderma.2005.03.013

Mahrt L, Ek M. 1984. The influence of atmospheric stability on potential evaporation. *Journal of Climate and Applied Meteorology* **23**(2): 222–234. DOI: 10.1175/1520-0450(1984)023<0222:TIOASO>2.0.CO;2

Mahrt L, Pan H. 1984. A two-layer model of soil hydrology. *Boundary-Layer Meteorology* **29**(1): 1–20. DOI: 10.1007/BF00119116

Mohanty BP, Shouse PJ, Miller DA, van Genuchten MT. 2002. Soil property database: Southern Great Plains 1997 Hydrology Experiment. *Water Resources Research* **38**(5). DOI: 10.1029/2000WR000076

Myneni RB, Hoffman S, Knyazikhin Y, Privette JL, Glassy J, Tian Y, Wang Y, Song X, Zhang Y, Smith GR, Lotsch A, Friedl M, Morisette JT, Votava P, Nemani RR, Running SW. 2002. Global products of vegetation leaf area and fraction absorbed PAR from year one of MODIS data. *Remote Sensing of Environment* **83**: 214–231. DOI: 10.1016/S0034-4257(02)00074-3

Naithani KJ, Baldwin DC, Gaines KP, Lin H, Eissenstat DM. 2013. Spatial distribution of tree species governs the spatio-temporal interaction of leaf area index and soil moisture across a forested landscape. *PLoS ONE* **8**(3): e58704. DOI: 10.1371/journal.pone.0058704

Nash JE, Sutcliffe JV. 1970. River flow forecasting through conceptual models. Part I: A discussion of principles. *Journal of Hydrology* **10**(3): 282–290. DOI: 10.1016/0022-1694(70)90255-6

Niu G-Y, Yang Z-L, Mitchell KE, Chen F, Ek MB, Barlage M, Kumar A, Manning K, Niyogi D, Rosero E, Tewari M, Xia Y. 2011. The community Noah land surface model with multiparameterization options (Noah-MP): 1. Model description and evaluation with local-scale measurements. *Journal of Geophysical Research* **116**: D12109. DOI: 10.1029/2010JD015139

Noilhan J, Planton S. 1989. A simple parameterization of land surface processes for meteorological models. *Monthly Weather Review* **117**(3): 536–549. DOI: 10.1175/1520-0493(1989)117<0536:ASPOLS>2.0.CO;2

Nutter WL. 1964. Determination of the head-discharge relationship for a sharp-crested compound weir and a sharp-crested parabolic weir. M.S. thesis, Department of Forest Hydrology, The Pennsylvania State University; 87.

Nyberg L. 1996. Spatial variability of soil water content in the covered catchment at Gårdsjön, Sweden. *Hydrological Processes* **10**: 89–103. DOI: 10.1002/(SICI)1099-1085(199601)10:1<89::AIDHYP303>3.0.CO;2-W

Pan HL, Mahrt L. 1987. Interaction between soil hydrology and boundary-layer development. *Boundary-Layer Meteorology* **38**(1): 185–202. DOI: 10.1007/BF00121563

Peters-Lidard CD, Pan F, Wood EF. 2001. A re-examination of modeled and measured soil moisture spatial variability and its implications for land surface modeling. *Advances in Water Resources* **24**(9): 1069–1083. DOI: 10.1016/S0309-1708(01)00035-5

Pokhrel P, Gupta HV. 2010. On the use of spatial regularization strategies to improve calibration of distributed watershed models. *Water Resources Research* **46**(1): W01505. DOI: 10.1029/2009WR008066

Qu Y. 2004. An integrated hydrologic model for multi-process simulation using semi-discrete finite volume approach. Ph.D. thesis, The Pennsylvania State University; 143.

Qu Y, Duffy CJ. 2007. A semidiscrete finite volume formulation for multiprocess watershed simulation. *Water Resources Research* **43**(8): W08419. DOI: 10.1029/2006WR005752

Rigon R, Bertoldi G, Over TM. 2006. GEOtop: a distributed hydrological model with coupled water and energy budgets. *Journal of Hydrometeorology* **7**(3): 371–388. DOI: 10.1175/JHM497.1

Saint-Venant B. 1871. Theory of unsteady water flow with application to floods and to propagation of tides in river channels. *Proceedings of French Academy of Science* **73**: 148–154.

Seghieri J, Galle S, Rajot JL, Ehrmann M. 1997. Relationships between soil moisture and growth of herbaceous plants in a natural vegetation mosaic in Niger. *Journal of Arid Environments* **36**: 87–102. DOI: 10.1006/jare.1996.0195

Shi Y, Davis KJ, Duffy CJ, Yu X. 2013. Development of a coupled land surface hydrologic model and evaluation at a critical zone observatory. *Journal of Hydrometeorology* **14**(5): 1401–1420. DOI: 10.1175/JHM-D-12-0145.1

Shi Y, Davis KJ, Zhang F, Duffy CJ. 2014. Evaluation of the parameter sensitivity of a coupled land surface hydrologic model at a critical zone observatory. *Journal of Hydrometeorology* **15**(1): 279–299. DOI: 10.1175/JHM-D-12-0177.1

Takagi K, Lin HS. 2012. Changing controls of soil moisture spatial organization in the Shale Hills Catchment. *Geoderma* **173–174**: 289–302. DOI: 10.1016/j.geoderma.2011.11.003

Van Genuchten MT. 1980. A closed-form equation for predicting the hydraulic conductivity of unsaturated soils. *Soil Science Society of America Journal* **44**(5): 892–898. DOI: 10.2136/sssaj1980.03615995004400050002x

Venables WN, Ripley BD. 2002. *Modern Applied Statistics with S*, 4th edn. Springer-Verlag: New York; 495.

Wallner M, Haberlandt U, Dietrich J. 2012. Evaluation of different calibration strategies for large scale continuous hydrological modelling. *Advances in Geosciences* **31**: 67–74. DOI: 10.5194/adgeo-31-67-2012

Western AW, Grayson RB. 2000. Soil moisture and runoff Processes at Tarrawarra. In *Spatial Patterns in Catchment Hydrology—Observations and Modelling*, Grayson RB, Blöshl G (eds). Cambridge University Press: New York; 209–246.

Western AW, Grayson RB, Green TR. 1999. The Tarrawarra project: high resolution spatial measurement, modelling and analysis of soil moisture and hydrological response. *Hydrological Processes* **13**(5): 633–652. DOI: 10.1002/(SICI)1099-1085(19990415)13:5<633::AIDHYP770>3.0.CO;2-8

Western AW, Zhou S-L, Grayson RB, McMahon TA, Blöschl G, Wilson DJ. 2004. Spatial correlation of soil moisture in small catchments and its relationship to dominant spatial hydrological processes. *Journal of Hydrology* **286**: 113–134. DOI: 10.1016/j.jhydrol.2003.09.014

Wösten JHM, Pachepsky YA, Rawls WJ. 2001. Pedotransfer functions: bridging the gap between available basic soil data and missing soil hydraulic characteristics. *Journal of Hydrology* **251**: 123–150. DOI: 10.1016/S0022-1694(01)00464-4

Wubbels JK. 2010. Tree species distribution in relation to stem hydraulic traits and soil moisture in a mixed hardwood forest in central Pennsylvania. M.S. thesis, Department of Horticulture, The Pennsylvania State University; 39.

Zreda M, Desilets D, Ferré TPA, Scott RL. 2008. Measuring soil moisture content non-invasively at intermediate spatial scale using cosmic-ray neutrons. *Geophysical Research Letters* **35**: L21402. DOI: 10.1029/2008GL035655